# Catalysis Science & Technology

Accepted Manuscript

ROYAL SOCIETY
OF CHEMISTRY

www.rsc.org/catalysis

Journal Name

ARTICLE

# Mapping reactivities of aromatic models with a lignin disassembly catalyst. Steps toward controlling product selectivity.†

Received 00th January 20xx,
Accepted 00th January 20xx

DOI: 10.1039/x0xx00000x

**www.rsc.org/**

Christopher M. Bernt,[a,‡] Giovanni Bottari,[b,‡] Jacob A. Barrett,[a] Susannah L. Scott,[a] Katalin Barta[b,*] and Peter C. Ford[a,*]

Copper-doped porous metal oxides catalyze the one-pot disassembly of biomass-derived lignin via C-O bond hydrogenolysis and hydrodeoxygenation in supercritical methanol. This catalytic system cleanly converts lignin as well as lignocellulose composites, such as sawdust, to organic liquids with little or no formation of intractable tars or chars. However, this catalyst based on Earth-abundant components also catalyzes less desirable aromatic ring hydrogenations and various methylations that contribute to the diversity of products. In this context, we undertook a quantitative experimental and computational evaluation of model reactions relevant to the reductive disassembly of lignin by this catalyst system in order to determine quantitatively the rates of desirable and less desirable chemical steps that define the overall product selectivities. Global fitting analysis methods were used to map the temporal evolution of key intermediates and products and to elucidate networks that provide guidelines regarding the eventual fates of reactive intermediates in this catalysis system. Phenolic compounds display multiple reaction pathways, but substrates such as benzene, toluene, and alkyl- and alkoxy- substituted aromatics are considerably more stable under these conditions. These results indicate that modifying this catalytic system in a way that controls and channels the reactivity of phenolic intermediates should improve selectivity toward producing valuable aromatic chemicals from biomass-derived lignin. To this end we demonstrate that the O-methylating agent dimethyl carbonate can intercept the phenol intermediate formed from hydrogenolysis of the model compound benzyl phenyl ether. Trapping the phenol as anisole thus gave much higher selectivity towards aromatic products.

## Introduction

Lignocellulose, the principal component of woody biomass, is a non-edible and sustainable feedstock that has the potential to be a renewable resource for producing commodity chemicals and fuels.[1-7] However, practical applications require an integrated approach to maximize atom and electron economy in extracting the energy and material contained therein. Lignocellulose is about 70-80% carbohydrates, with the balance largely being lignin. The latter is a complex, heterogeneous polymer (Figure 1) formed biologically by free radical initiated polymerization of aromatic monolignols (principally p-coumaryl, coniferyl and sinapyl alcohols) in ratios that depend upon the source.[8] The principal linkages are aryl-ether bonds, although the monolignols are occasionally crosslinked by C-C bonds. Notably, lignin has the highest relative carbon content of the major lignocellulose components and represents a greatly underdeveloped renewable resource for producing aromatic chemicals.[1-3] However, biorefineries for "2nd generation" ethanol fuel production typically focus on the carbohydrates, and the lignin fraction, owing to its chemical recalcitrance and heterogeneity, is mostly burned to produce low-grade heat.[1] This is also the case with the production of paper goods from lignocellulose. Thus, designing selective pathways to convert lignin to chemicals and/or liquid fuels should add considerable value to biomass conversion schemes.

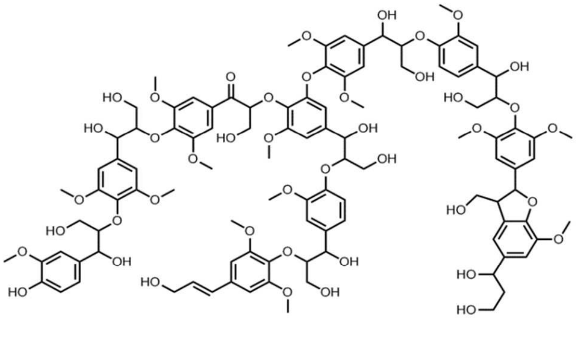

**Figure 1.** A representative structure for a lignin fragment based upon structural data by Tuskan et al. and Mansfield et al.[9,11]

---

[a] *Department of Chemistry and Biochemistry and the Center for the Sustainable Use of Renewable Feedstocks, University of California, Santa Barbara, Santa Barbara, California 93106-9510, USA.*

[b] *Stratingh Institute for Chemistry, University of Groningen, Nijenborgh 4, 9747 AG Groningen, The Netherlands.*

† Electronic Supplementary Information (ESI) available. Description of the algorithms used to convert quantitative GC data to product amounts and tables summarizing analysis of the temporal evolution of products from reactions of individual substrates over the Cu-doped PMO catalyst.See DOI: 10.1039/x0xx00000x

‡ These authors contributed equally to this work.

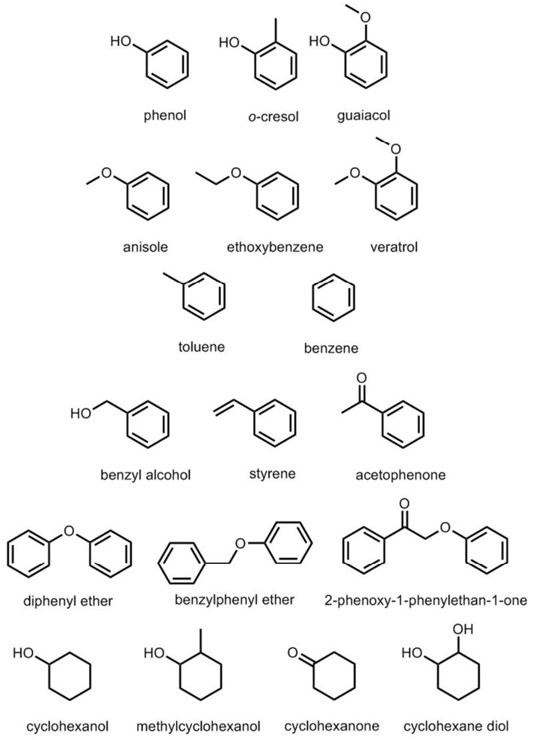

**Figure 2.** Aromatic model compounds studied representing phenyl ether linkages and types of functional groups anticipated as intermediates in reductive lignin disassembly.

It is estimated[1,10] that 62 Mt residual lignin will be generated annually by 2022 from US-mandated ethanol production alone. This is on the same scale as BTX (benzene, toluene and xylenes) production from fossilized carbon.[11] While BTX could be a drop-in target for biomass conversion, lignin disassembly will also lead to functionalized aromatics that have the potential to serve as the building blocks for new materials.[12] Effective utilization of lignin remains a major intellectual challenge[1-3] that is drawing increasing interest from the chemical community.[13-20]

Our laboratories previously demonstrated the clean reductive disassembly of organosolv lignin to organic liquids without formation of intractable chars or tars.[21] This process is heterogeneously catalysed by a copper-doped porous metal oxide (Cu20PMO) that is prepared by calcining a 3:1 $Mg^{2+}$:$Al^{3+}$ hydrotalcite in which 20% of the $Mg^{2+}$ had been replaced by $Cu^{2+}$. The reaction is carried out in a batch reactor in super-critical methanol (sc-MeOH). The same catalytic system also liquefies cellulose and, remarkably, disassembles lignocellulosic materials such as sawdust or wood chips to organic liquids with little or no char formation.[22,23] A relatively complex mixture of aliphatic alcohols and ethers is obtained from the carbohydrate fraction, while a similarly complex mixture of propylcyclohexanol derivatives is generated from the lignin.[21,22] The latter products are attributed to the hydrogenolysis of various phenyl ethers, with competing and subsequent hydrodeoxygenation (HDO) and hydrogenation of alkenes and aromatic rings. The methanol medium provides the reducing equivalents[21-24] via alcohol reforming[25] and the water-gas shift reaction,[26] both catalysed by the Cu-PMO to generate a gas phase consisting of $H_2$ and CO plus some $CO_2$ and small amounts of methane. Less desirable side-reactions in this medium are ring methylations. These processes and the composition of the gas phase products were described in greater detail previously.[21-24]

The importance of the copper in these catalysts was demonstrated in our earlier studies with pine sawdust.[22] While this substrate was readily converted to organic liquids by the Cu20PMO in sc-MeOH, the products are largely char and unreacted biomass under similar conditions with a Mg/Al hydrotalcite-derived PMO catalyst not containing copper. Analogous results were found when no catalyst was added.

Cu-doped PMO catalysts were subsequently shown to be effective in the $H_2$ hydrogenation of candlenut lignin to aromatic products[27] and for the reduction of 5-hydroxymethylfurfural to tetrahydrofuran derivatives.[28,29] A related study recently demonstrated disassembly of organosolv lignin using a copper-doped magnesium-aluminum mixed metal oxide catalyst in supercritical ethanol.[30] However, it is clear that improved selectivity to generate product streams composed of a limited number of aromatic chemicals would significantly enhance the value of lignin as a renewable feedstock.

In these contexts, we describe here a reactivity study of various small molecules (Figure 2) that have structures/functional groups representative of the key reactive intermediates anticipated during lignin disassembly by Cu-PMO catalysts in sc-MeOH. Global kinetics analysis of the resulting reaction pathways allows mapping the reaction networks for the expected intermediates. Such networks can provide valuable insight into the underlying disassembly mechanisms and side-reactions that strongly influence the selectivity of this catalytic process as well as guidelines for intercepting the responsible intermediates, hence improving selectivity. Note that Gates and coworkers[31,32] have used a different numerical method to generate analogous reaction networks for the platinum catalysed reactions of $H_2$ with vaporized models for pyrolysis-derived bio-oils.[6,33-35]

## Experimental Section

**Materials:** Methanol was purchased from Fischer and dried over molecular sieves. Model compounds used in reactivity studies were purchased from Sigma and used without further purification. Copper-doped porous metal oxide catalysts were prepared from 3/1 $Mg^{2+}$/$Al^{3+}$ hydrotalcites with 20 mol% of the $Mg^{2+}$ replaced by $Cu^{2+}$. Prior to use, the catalysts were calcined at 460 °C for 24 h.[21,22,24] Un-doped PMO catalysts used in control studies were prepared by calcination of 3/1 $Mg^{2+}$/$Al^{3+}$ hydrotalcite purchased from Sigma.

**Reactivity Studies:** Catalysis studies were conducted in high pressure, stainless steel mini-autoclave batch reactors consisting of 3/4-inch Swagelok unions capped by two 3/4 inch Swagelok plugs (see Fig. 4 of ref. 18). The total volume of these mini-reactors is 10 mL. Typically, catalyst samples (50 or 100 mg), the organic substrate (1 mmol) and the internal reference decane (20 µL) plus dry methanol (3 mL) were sealed in the mini-reactor using a torque wrench. For reactions with dimethyl carbonate, 1 mL of the methanol was replaced with DMC. Catalysis runs were conducted by placing a set of these mini-reactors (typically 4 to 8) with identical mixtures into a heating block mounted in a furnace set at the chosen temperature (typically 310 °C).

After a designated time interval (0.5-18 h), a reactor was removed from the oven and quenched by rapid cooling in a room temperature water bath or ice bath. The built-up gases (which analyze as a mixture of $H_2$, CO, $CO_2$ and some methane)[22] were then released, and the remaining contents of the vessel were transferred to a 15 mL, disposable centrifuge tube. (**Warning**: the high pressures usually produced during a mini-reactor experiment require extreme caution in handling). The reactor was then rinsed with MeOH (4 mL), and combined with the original contents. The tube was centrifuged at 6500 g for 15 min. to separate the liquid and solid fractions. The liquid contents were collected from the tube, and the remaining solid was suspended in another 3 mL volume of MeOH, which was centrifuged to separate liquid and solid. The additional MeOH was intended as a wash to extract residually adsorbed substrate and soluble products. (The earlier studies with organosolv lignin and lignocellulose composites as substrates[21,22] showed negligible or no gain in the mass of the recovered catalyst after such treatment indicating little organic residue, including chars, on the Cu20PMO.) The two liquid fractions were combined for analysis by GC-MS and/or GC-FID techniques. In this way, the temporal evolution of each component was determined, with each time point representing a semi-independent experiment.

Product analysis was performed primarily by gas chromatography with flame ionization or mass spectral detection. GC-MS measurements were taken on a Shimadzu GC-2010 gas chromatography coupled to a Shimadzu GCMS-QP2010 mass spectrometer. Samples of 1 µL volume were injected at a temperature of 225 °C in split mode with a 200:1 ratio. This instrument was equipped with a 30 m x 0.25 mm Agilent DB-1 column with a 0.25 µm dimethylpolysiloxane lining. The GC program was run in pressure flow control mode at 40 kPa, 162.3 mL/min total flow, 0.79 mL/min column flow, a linear velocity of 32.5 cm/sec and a purge flow of 3.0 mL/min. The column temperature program started with a hold at 60 °C for 2 min. followed by a 25 °C/min ramp up to 200°C where the temperature was held for 4 min. The corresponding MS program had an ion source temperature at 250 °C, interface temperature at 230 °C and recorded from 2.0 to 11.6 min. during the GC program.

**Quantitative measurements:** GC-FID measurements were conducted on an Agilent/HP 6890N (G1530N) gas chromatograph equipped with a flame ionization detector. This GC-FID instrument was operated with two different columns. When used with a 30 m x 0.25 mm Agilent DB-1+DG column, with a 0.25 µm dimethylpolysiloxane lining and a guard column, 0.5-2 µL samples were injected at a temperature of 225 °C in split mode with a 200:1 ratio. With this column, the GC program was run in pressure flow control mode at 104.8 kPa, 276 mL/min total flow, 1.4 mL/min column flow, a linear velocity of 32 cm/sec and a purge flow of 3.0 mL/min. The temperature program started with a hold at 50 °C for 2 min. followed by a 25 °C/min ramp up to 200 °C where the temperature was held for 2 min. When used with a 30 m x 0.25 mm Agilent DB-5 column with a 0.25 µm (5%-phenyl)-methylpolysiloxane lining, 0.5-2 µL samples were injected at a temperature of 250 °C in split mode with a 20:1 ratio. With this column, the GC program was run in pressure flow control mode at 68.1 kPa, 27.6 mL/min total flow, and a 0.70 mL/min column flow. The FID detector was set at 250 °C with 30 mL/min $H_2$ and 350 mL/min air flow. The temperature program started with a hold at 45 °C for 6 min. followed by a 4 °C/min ramp up to 175 °C where the temperature was held for 10 min.

Further quantitative measurements were performed on a Hewlett Packard 5890 GC-MS-FID. The GC is equipped with a 60 x 0.25 mm i.d. and 0.25 µm Restek RTX-1701 film capillary column and a 1:1 split ratio to the MSD and FID was set. Temperature of injector and detector were set at 250 °C and 285 °C, respectively. The temperature program starts from 40 °C (10 min) and is then increased up to 250 °C with a heating rate of 10 °C/min.

The data reported for individual products were drawn from these quantitative GC-MS or GC-FID experiments and converted to µmoles using stand curves or algorithms set forth by Scanlon and Willis as described in the Supporting Information (SI).[36]

**Global Fitting and Kinetics Analysis:** The initial design of reaction networks was based on the most parsimonious application of previously observed PMO catalysed reactivities: hydrogenation, hydrodeoxygenation, C-O bond hydrogenolysis and methylation. Reactions were assumed to be first order with respect to the substrate reactant at each step. Refinements to the model were based on the results of global fitting to the proposed models. Global fitting was performed using DynaFit version 4.05.087 software on a desktop computer (BioKin Ltd.).[37]

## Results and Discussion

Once the aryl-ether bonds are cleaved by hydrogenolysis or solvolysis during lignin disassembly, a series of molecular intermediates are generated.[21] Expected cleavage products are phenolics with various substitution patterns on the aromatic ring including methoxy and oxidized aliphatic groups. In order to channel these intermediates into desirable and selective product streams, it is necessary to evaluate their reactivities under the conditions relevant to catalytic depolymerization. The simple models representative of those moieties (Figure 2) include mono-oxygenated (phenol and anisoles) and di-oxygenated (guaiacol and veratrol) aromatics that are common lignin motifs and disassembly intermediates, several other typical aromatic types (toluene, benzyl alcohol, styrene and acetophenone), as well as products of aromatic hydrogenation (cyclohexanol and cyclohexanone). Several di-aromatic model compounds were also investigated in order to probe the rates of the sequential processes following aromatic ether hydrogenolysis.

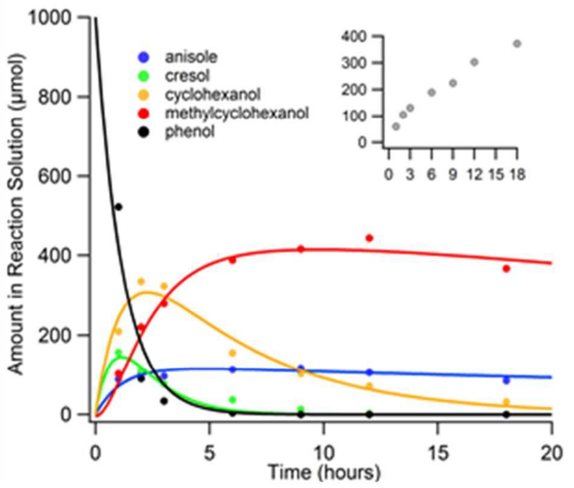

**Figure 3.** Temporal evolution of products formed from phenol (1 mmol) in a batch reactor containing Cu20PMO in sc-MeOH. (T = 310 °C) *Inset*: sum of the other products not shown in parent graph (see SI). Material balance 78% after 6 h and 75% after 18 h.

contained substrate (1.0 mmol), Cu20PMO catalyst (100 mg) and MeOH (3.0 mL). Decane (20 µL) was also added as an internal standard for quantification. A typical run involved 7-8 of these mini-reactors with identical quantities of catalyst, substrate and solvent that were heated together in an oven at the defined temperature (typically, 310 °C). At different time intervals, reactors quenched to room temperature in a water bath, and the products were analysed using GC-MS fragmentation patterns for identification and GC-FID and GC-MS integrated areas for quantification.

Under this catalytic system the solvent contributes to the product mass by both methylation and hydrogenation so it is more appropriate in this case to consider the molar material balance of substrate derived products. In the present study the material balance over the course of catalysis was greater than 90% for most substrates, including the less reactive dimer diphenyl ether. The experiments with lower molar balance were those with phenolic substrates and those that lead to phenolics as major intermediates. In those cases, the product spread gave numerous small peaks that could be identified in most cases but were too small to quantify reliably, so lower molar balances are largely attributed to product proliferation. Details for specific substrates are included in the Supporting Information. In the kinetics analysis, unaccounted products were treated as undefined product sinks. The temporal data thus obtained and summarized in SI tables were evaluated by global kinetics analysis using the DynaFit software[37] to give reactivity networks describing the interconnected catalytic pathways of different substrates and expected intermediates. The fits described in this study are sufficient to explain the defining trends in the observed data. A more detailed discussion on the descriptive statistics of these fits can be found in the SI.

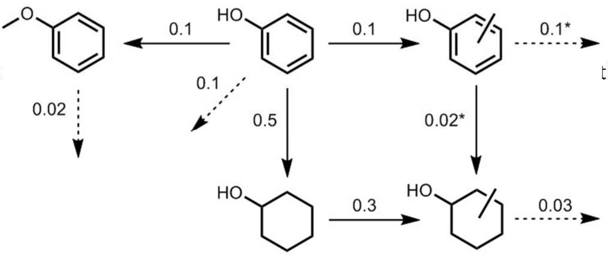

**Scheme 1.** Reaction network for phenol: (1 mmol substrate, 100 mg Cu20PMO, 3 mL MeOH, 310 °C). Observed rate constants are shown for each step, in units of $h^{-1}$. Dashed lines indicate conversion to unidentified compounds. Asterisks indicate rate constants fixed based on independent investigation of reaction products.

**Reactions of aromatic alcohols phenol and guaiacol:** The time course of major products from phenol over an 18 h period is shown in Figure 3 and summarized in SI Table S-1. After just 1 h at 310 °C, roughly half the phenol was consumed. After 3 h, this increased to 92%. The major products at this time were methylcyclohexanol (25%), cyclohexanol (28%), anisole (9%) and 2-methylphenol (7%). Lesser products included dimethylphenols (3%), dimethylcyclohexanols (3%), 2-methylanisole (2%), 2-methylcyclohexanone (1%), cyclohexanone (1%), methoxycyclohexane, methylcyclohexane, cyclohexane and others. For reaction times ≥9 h, the major product(s) were methylated cyclohexanols (MCHs), while anisole was the most abundant aromatic product. *These products suggest that phenol is depleted via three primary reaction channels*: (i) reduction to cyclohexanol, (ii) methylation of the aromatic ring to give cresols (methylphenols) and (iii) methylation at oxygen to form anisole. Subsequent reactions convert the primary product cyclohexanol to MCHs (Scheme 1). Ring methylation is a common reaction for phenols,[38] and was shown to be a major pathway in earlier studies with the model compound dihydrobenzofuran (DHBF) under comparable conditions.[24]

The reactivity of phenol under analogous conditions but with a PMO catalyst derived by calcining Mg/Al (3/1) hydrotalcite without copper was nearly two orders of magnitude slower. After 18 h, GC analysis showed that 68% of the phenol was still present, the remainder being anisole (12%), cresol (2%) some unidentified lower retention time (RT) species thought to be monomers (<1%) and higher RT products that were dimeric (5%) (see SI Table S-1b). These products are consistent with the findings of Crocella et al.[38]

Global kinetics analysis of the temporal profiles for phenol reactions resulted in the reactivity network in Scheme 1. As will be evident below, these results show that phenol is particularly susceptible to aromatic hydrogenation under the catalytic conditions.

As shown in Scheme 1, there are two likely routes to methylcyclohexanol from primary phenolic products: methylation of cyclohexanol and hydrogenation of cresol. To verify the rates of these secondary reactions, separate sets of

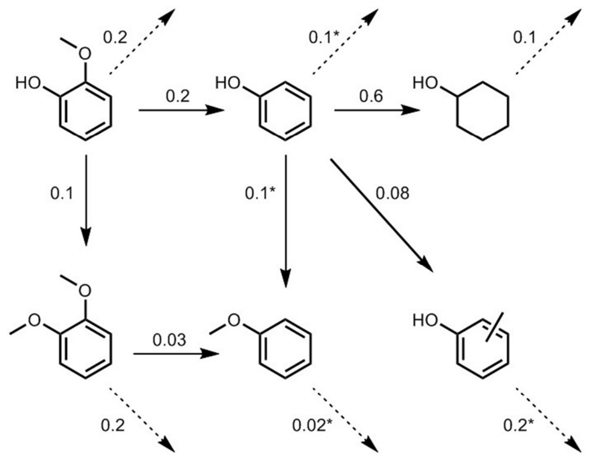

**Scheme 2.** Reaction network for guaiacol. See scheme 1 for reaction details.

experiments were carried out for cyclohexanol and for cresol. The results of the cyclohexanol experiment are described below, and the detailed results with cresol can be found in the Supporting Information (SI Table S-2). In the case of cresol, more than half (51%) was consumed after four hours. Of the total mixture after 4 h, dimethylphenol (xylenol) was the major product (33%) followed by methylcyclohexanol (6%) and methylmethoxybenzene (5%). These results indicate that ring methylation significantly slows the hydrogenation of the phenolic derivative. Thus, the principal products from the long-term reaction of phenol under the described conditions are MCHs formed by methylation of the cyclohexanol(s) resulting from phenol hydrogenation.

In analogy to phenol, guaiacol (2-methoxyphenol) displayed more complicated reaction sequences under these conditions. The most important initial steps were methylation of the phenolic oxygen to give veratrol (dimethoxybenzene), and hydrogenolysis of the $C_{aryl}$-$OCH_3$ bond to give phenol. After 3 h, guaiacol was largely (92%) consumed, with the major products being veratrol (18%), cyclohexanol (15%), cyclopentylmethanol (14%) and phenol (11%). Lesser products that are likely derived from those formed initially are cyclohexanediols (11%), methylcyclohexanols (5%), 2-methoxy-4-methylphenol (methyl anisole) (5%), dimethylcyclohexanol (4%), dimethylphenols (2%), 2-methoxycyclo-hexanone (3%), anisole (2%) as well as others (see SI Table S-3). Although not observed as an intermediate by GC-MS analysis, catechol is a likely intermediate species, given the appearance of both 1,2cyclohexanediol and cyclopentylmethanol in the final reaction mixture consistent with mechanisms proposed by Deutsch and Shanks,[39] as well as by Lercher *et al.*[40] Scheme 2 illustrates the key steps for the substrate guaiacol, deduced by the kinetics analysis.

**Alkoxy aromatics:** Both anisole (methoxybenzene) and ethoxybenzene proved to be dramatically less reactive than phenol or guaiacol under typical catalysis conditions. Notably, ring hydrogenations were observed to a much smaller extent than with the phenolics, and the predominant pathway was aromatic ring HDO.

For anisole, only 5 % of the substrate was consumed in the first 3 h. Notably, the primary product (by far) was benzene, formed by $C_{aryl}$-OMe bond hydrogenolysis. The others (cyclohexanol, 2-methyl-cyclohexanol and methylcyclohexane) apparently result from $CH_3$-O bond hydrogenolysis followed by reactions of the intermediate phenol. At longer reaction times (6 h), a modest amount of the ring-hydrogenated methoxy-cyclohexane (~2%) was also observed (see SI Table S-4).

Similarly, ethoxybenzene showed preferential hydrogenolysis of the $C_{aryl}$-OEt bond, affording the HDO product benzene as the major product, and a low rate of ring hydrogenation (3% after 6 h). After 6 h, only 12% of this substrate was consumed. The products were benzene (6%), ethoxycyclohexane (3%), cyclohexanol (1%), 2-methyl-cyclohexanol (0.7%) and several unknowns (see SI Table S-5).

Veratrol (1,2-dimethoxybenzene) proved to be considerably more reactive than anisole; however, the principal pathway is aromatic HDO to give anisole and not ring hydrogenation. After 3 h, 52% was consumed; after 12 h, this rose to 97%. The predominant product was anisole (40% after 3 h), apparently formed via $C_{aryl}$-OMe bond hydrogenolysis. The anisole yield peaked at ~12 h then diminished, very likely owing to slow hydrogenolysis to benzene and hydrogenation to methoxycyclohexane. Other products after 3 h included cyclohexanol (3%), 2-methylcyclohexanol (3%), benzene (2%), dimethyl-cyclohexanol (1%), methoxycyclohexane (1%) and cyclohexane (0.9%) (see SI Table S-6). Direct hydrogenation to 1,2-dimethoxycyclohexane was not observed.

**Simpler aromatics and those with pendant functional groups:** The oxygen-free aromatics benzene and toluene displayed very little reactivity under the conditions effective for catalytic lignin disassembly. For example, when toluene was the substrate, 99% remained after 3 h at 310 °C. Methylcyclohexane (1%) was the only product detected. Benzene was similarly unreactive (2% conversion to cyclohexane after 3 h).

In contrast, benzyl alcohol proved to be quite reactive (full conversion after 3 h), but primarily toward HDO, as illustrated in eq. 1. Toluene was the principal product (>98%), but small amounts of methylcyclohexane and cyclohexylmethanol were also found. While traces of an unidentified product were also seen, ring methylation clearly plays a very minor role and hydrodeoxygenation of the benzylic OH is the main pathway, in line with the earlier findings.[39]

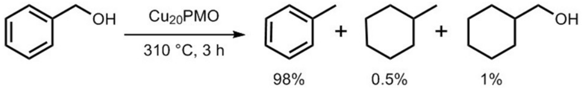

(1)

Styrene is also very reactive, but solely toward vinyl hydrogenation to give ethyl benzene selectively (>99% after 3 h). Traces (< 1%) of ethylcyclohexane were found, but no ring methylation products were detected

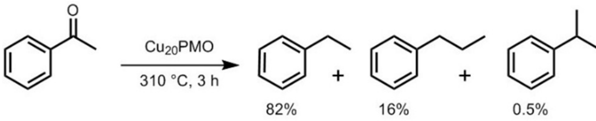

(2)

Under analogous conditions, acetophenone (acetylbenzene) also gave full conversion after 3 h; the primary pathway was the formation of ethylbenzene (82%) (eq. 2), which likely took place via ketone hydrogenation to 1-phenylethanol, followed either by direct hydrogenolysis of the C-OH bond or by dehydration to styrene, then hydrogenation. Another significant product was n-propylbenzene (16%), presumably the result of acetyl group methylation (perhaps via the enol isomer) followed by HDO. Interestingly, sec-butylbenzene was also identified as a minor (0.5%) product.

**Model compounds with two aromatic rings:** Three such compounds were investigated: diphenyl ether (DPE), benzyl phenyl ether (BPE) and 2-phenoxy-1-phenylethane-1-one (**1**).

DPE proved to be more reactive than anisole or ethoxybenzene, but much less so than phenol, guaiacol or veratrol. After 3 h, 23% was consumed. The first hydrogenolysis step of DPE would give equal amounts of benzene and phenol. Accordingly, benzene was 48% and phenol 4% *of the breakdown products.* The other products, cyclohexanol (28%), 2-methylcyclohexanol (15%) and much smaller quantities of anisole (2%), cyclohexane (1%) and dimethylcyclohexanol (1%), can largely be attributed to subsequent reactions of the phenol intermediate (Scheme 3).

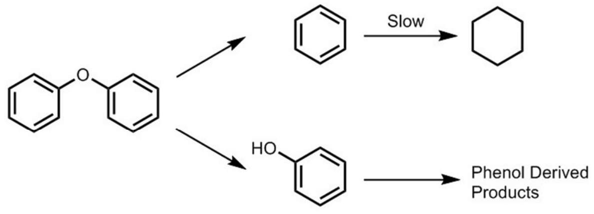

**Scheme 3.** Observed pathway for diphenyl ether (DPE).

BPE proved much more reactive. With only 50 mg catalyst, this substrate was about 85% consumed after only 1 h, and none was left after 3 h. Carbon-oxygen bond hydrogenolysis of BPE should lead either to benzene plus benzyl alcohol or to toluene plus phenol, depending upon which C-O bond is cleaved.

The data summarized in Figure 4 (see SI Table S-7) show that toluene is formed immediately in nearly stoichiometric quantities, while the other principal (initial) product is phenol. Thus, the predominant first step is $C_{benzyl-O}$ hydrogenolysis. As expected, the phenol is consumed by subsequent reactions (Scheme 4) giving (mostly) non-aromatic products.

As with phenol, the reactivity of benzyl phenyl ether under analogous conditions over 3:1 Mg/Al PMO proved to be considerably less than over Cu20PMO (see SI Table S-7b). These reactions also indicated a very different product progression. Ether cleavage was an order of magnitude slower, with 41% of the BPE unreacted after 6 h. Thus, the clean ether hydrogenolysis, which is a hallmark of Cu20PMO, is indeed dependent upon the copper dopant. Surprisingly some toluene is formed, but unlike the case with CuPMO, this did not appear concurrently with the loss of the BPE, but later, indicating that is a secondary product. Longer RT products shown by GC-MS to be other dinuclear species were also formed. A possible mechanism could be analogous to the one described by Pelzer et al.,[41] where hydrolysis (made possible by residual water) converts BPE to phenol and benzyl alcohol. The poor material balance at longer reaction times and the higher molecular weight products are consistent with the pathways proposed by Pelzer et al. Given that the undoped PMO is ineffective in lignin disassembly, the origins of these secondary reactions were not pursued further. Since the reactions with the undoped PMO are considerably slower, they would not have a significant effect on the global fitting kinetics analyses of the primary reactions seen with Cu20PMO.

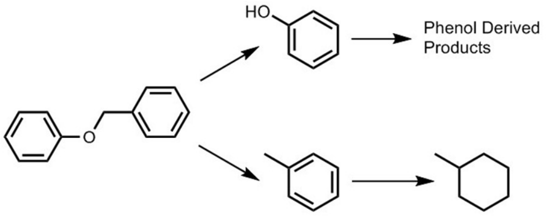

**Scheme 4**. Observed reaction pathways for benzyl phenyl ether.

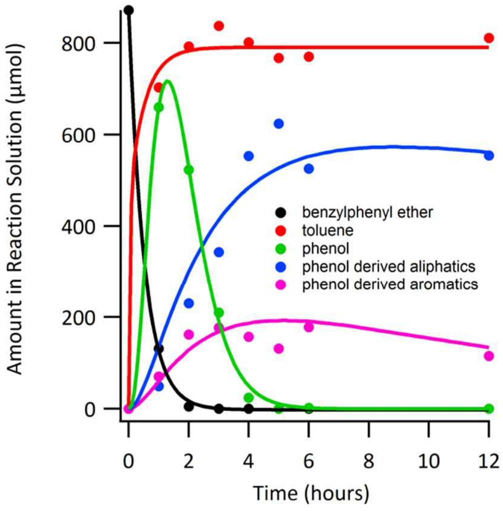

**Figure 4.** Temporal evolution of products during Cu20PMO-catalyzed reactions of benzyl phenyl ether (ca. 1 mmol). Total material balance was 82% after 18 h.

On turning to 2-phenoxy-1-phenylethane-1-one (**1**), the above studies offer some expectations regarding reaction pathways for this more complex substrate. Based on the results for acetophenone and of benzyl phenyl ether, one would expect the two fastest reactions for **1** (1000 μmol) to be carbonyl group hydrogenation to give 2-phenoxy-1-phenylethanol (**2**) (pathway (a) in Scheme 5) and direct hydrogenolysis of the $CH_2$-O bond to give acetophenone and phenol (pathway b).

Subsequent hydrogenolysis of **2** would first give 1-phenyl ethanol plus phenol, and rapid HDO of the former would give ethylbenzene. Notably, ethylbenzene (600 mmol) represents the most plentiful product from **1** under these conditions (SI Table S-8), but it is notable that both pathway (a) and (b) predict this product given the expected reactivities of the respectively proposed 1-phenylethanol and acetophenone intermediates. The substantial quantities of 2-methylcyclohexanol (350 µmol) and cyclohexanol (250 µmol) products point toward phenol as a reactive intermediate.

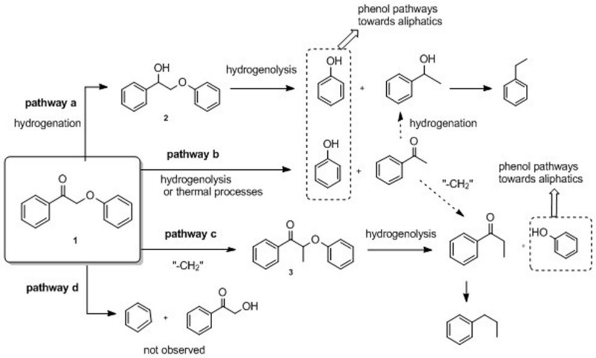

**Scheme 5.** Likely steps in disasembly of 2-phenoxy-1-phenylethan-1-one (1)

Notably, the second most plentiful product after ethylbenzene is propylbenzene (300 µmol, SI Table S-8), and this can best be explained by pathways (b) or (c). In pathway (b), the acetophenone intermediate might undergo methylation and subsequent HDO of the formed propyl-phenyl ketone. Indeed, this product was also observed when acetophenone was used as substrate. Alternatively, it appears that **1** might undergo facile methylation of the methylene adjacent to the carbonyl (pathway c) to give compound **3,** in analogy to the reaction proposed for acetophenone. Once formed, **3** could undergo steps analogous to pathways (a) or (b) to give propylbenzene plus phenol-derived products.

Pathway (d), the scission of the phenyl ether bond to give benzene, would not be not expected given the reactivity pattern seen for benzyl-phenyl ether. This suggestion was confirmed by the observation of very little benzene in the product mixture (Table S-8); thus, (d) must play at most a minor role.

**Aliphatic alcohols and ketones:** The above di-aromatic model compounds as well as oxygenated simple aromatics have provided ring hydrogenation products, mainly cyclohexanol, which originates from phenol hydrogenation. Thus, the reactivities of such derivatives were further investigated to probe the origin of major products such as the methylcyclohexanols.

Cyclohexanol, the expected result of phenol hydrogenation, proved to be quite reactive. Analysis after 1 h reaction under the standard conditions found that 12% of that substrate was consumed; after 3 h, this increased to 36%. Methylated cyclohexanol was by far the dominant product initially formed (Figure 5). (SI Table S-9).

2-Methylcyclohexanol was somewhat less reactive than cyclohexanol with only 19% being consumed after 3 h. The principal products were dimethylcyclohexanols (13%) 2-methylcyclohexanone (3%), methylcyclohexane (1%), 2-methyl-1-methoxycyclohexane (0.6%) and unknowns (<2%).

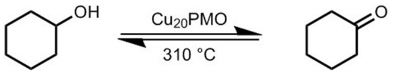

(3)

The formation of a cyclohexanones as minor products in several cases suggests that the cyclohexanols undergo reversible dehydrogenation to the ketone analogs (eq. 3), followed by methylation at the β-carbon. If so, cyclohexanone itself should be very reactive toward ring methylation as well as to (reversible) ketone hydrogenation. This proved to be the case when cyclohexanone was used directly as the substrate. After 3 h, the starting material was mostly consumed, and the product mixture contained 2-methylcyclohexanol (55%), cyclohexanol (22%) and dimethylcyclohexanols (13%) and the lesser products, 2-methylcyclohexanone (2%), methylcyclohexane (2%) and cyclohexane (1%).

Not surprisingly, a mixture of cis- and trans-1,2-cyclohexanediol gave an even larger collection of products Of particular interest was the ring contraction product cyclopentylmethanol (12%), which is possibly the result of a pinacol rearrangement.[39,40] The same product was seen when guaiacol was the substrate (see above).

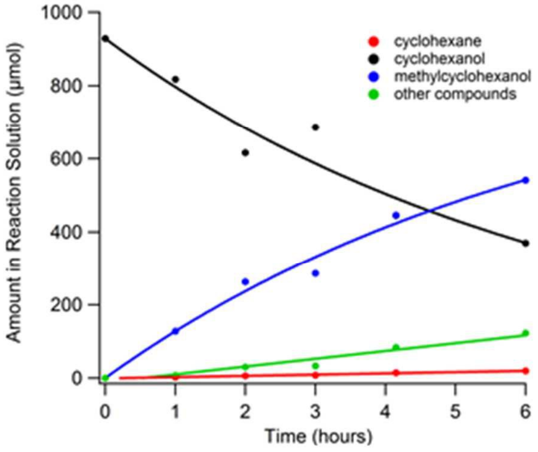

**Figure 5.** Temporal evolution of products formed from cyclohexanol (ca. 1mmol) in a batch reactor containing Cu20PMO in sc-MeOH. (T = 310 °C). Total material balance was greater than 99% after 6 hours.

### Overview of kinetics results

Scheme 6 is a comprehensive reactivity network compiled from the most significant individual networks described above, while Table 1 compares calculated rate constants in terms of reaction and substrate types (a more detailed network is given in SI Figure S-1). The *k*'s determined for individual steps and measured for different initial substrates are statistically self-consistent. Not only does this allow for comparisons across the whole network, but it is also an indicator that any competitive effects to the observed kinetics under these conditions must be minimal. Such global quantification thus allows one to identify key pathways leading toward or away from the desirable aromatic products when this catalytic system is employed for lignin disassembly.

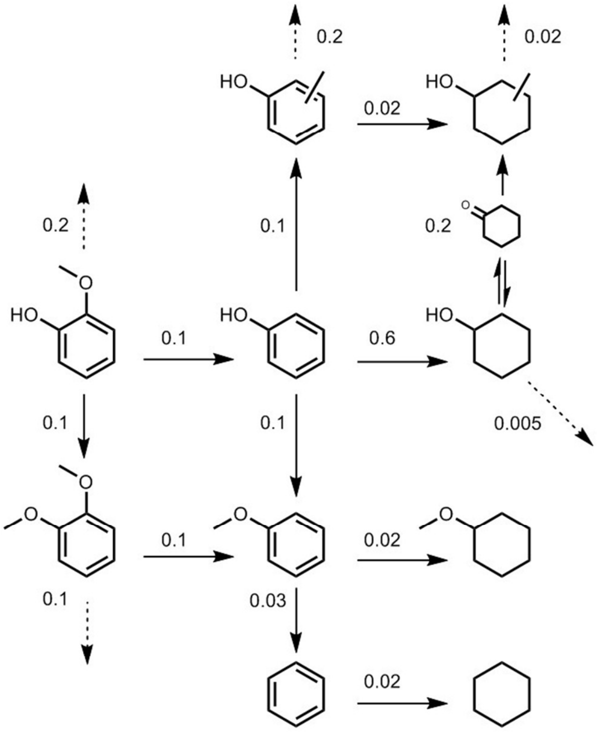

**Scheme 6.** Reaction network for simple mono-aromatic lignin model compounds over Cu20PMO.

**Table 1:** Overview of $k_{obs}$ trends observed with 1 mmol substrate, 100 mg Cu20PMO, and 3 mL MeOH, at 310 $^{o}$C

| Qualitative Rate | $k_{obs}$ ($h^{-1}$) | Reactions |
|---|---|---|
| Fastest | > 1.0 | Benzyl phenyl ether hydrogenolysis |
| | | Styrene hydrogenation |
| | | Benzylic alcohol hydrodeoxygenation |
| Fast | 0.75 - 0.2 | Phenolic hydrogenation |
| | | Cyclohexanol methylation |
| Slow | 0.10 - 0.05 | Phenolic methylation |
| | | Cresol methylation |
| Slowest | <0.05 | Other aromatic hydrogenation |
| | | Aryl phenoxy hydrogenolysis |
| | | Phenolic hydrodeoxygenation |

For example, hydrodeoxygenation via hydrogenolysis is quite fast with benzylic alcohols, but much slower with the cyclohexanols or phenol. For phenol, ring hydrogenation and methylation are the dominant pathways. In contrast, these are suppressed for anisole and ethoxybenzene to the point where slow HDO to the even less reactive benzene is the most significant reaction. Ring methylation of phenols contributes to product proliferation. However, since cyclohexanols are end-products of phenolic hydrogenation, the relatively fast methylations of the latter (via a cyclohexanone intermediate) have a major impact on product distributions.

### Reaction of BPE in methanol/dimethyl carbonate

Comparisons across the reactivity network provide valuable insight into improving the catalytic selectivity. Since phenolic derivatives are inevitable outcomes of reductive lignin disassembly, one must address the facile ring hydrogenation and methylation of these species in order to enhance the yield of aromatics. Possible scenarios might include designing a HDO co-catalyst to be very active toward phenols,[34] modifying the catalyst composition to suppress phenolic hydrogenation, or chemically trapping such intermediates. The third approach was investigated by using dimethyl carbonate (DMC), a known O-methylating agent that is activated Mg/Al metal oxides,[42-44] as a cosolvent.

The reaction with BPE as the substrate was run under otherwise typical conditions in a solution prepared with 2 mL MeOH and 1 mL DMC. After 1 h, the benzyl phenyl ether was 89% consumed, with the concurrent production of toluene, phenol and anisole (Figure 6). Also found were traces of cresols and aliphatic compounds previously shown to be derived from phenol. By 6 h, the BPE was completely converted with the primary products being toluene (900 µmol) and anisole (490 µmol); thus, O-methylation of phenol channelled the products away from ring hydrogenation.

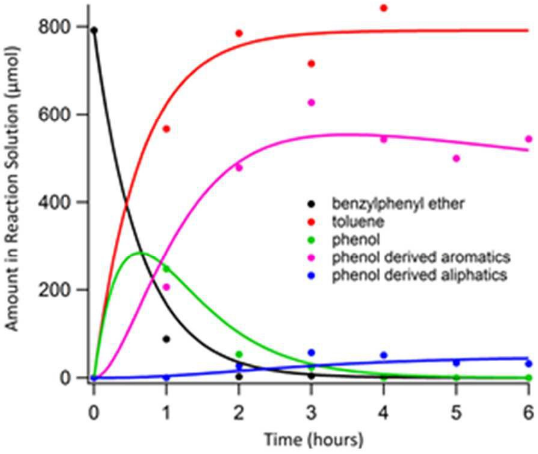

**Figure 6**. Temporal product evolution for the reactions of benzyl phenyl ether in 2:1 MeOH:dimethyl-carbonate over Cu20PMO (300 $^{o}$C). Material balance was 93% after 18 hours.

The reactivity network in Scheme 7 was drawn from the temporal evolution of products shown in Figure 6. Thus, it is clear that the percentage of phenol-derived aromatics, mostly in the form of anisole, is dramatically higher than observed in methanol alone (Figure 4) under comparable conditions.

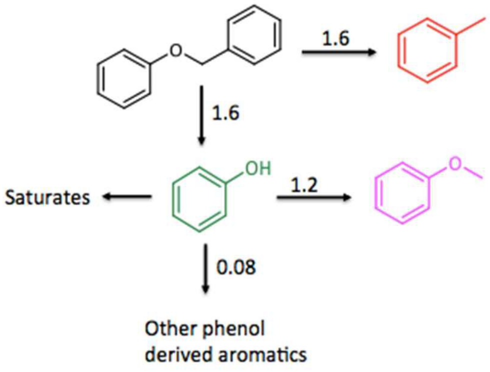

**Scheme 7.** Reactivity network for benzyl phenyl ether with Cu20 PMO in 2:1 MeOH:DMC (300 °C).

Since the mini-reactor experiments summarized in Figure 6 have less methanol (2 mL) than was used to gather the data described in Figure 4, we deemed it important to compare two systems containing the same quantities of MeOH. Figure 7 illustrates the product yields determined by GC-FID for the reactions of BPE over Cu20PMO after side-by-side reaction for 12 h under identical conditions, one with only 2 mL of MeOH as solvent the other with 3 mL of 2:1 MeOH:DMC. Clearly the aromatics yield proved dramatically higher in the latter case owing largely to the interception of the phenolic intermediates. In another control experiment, the reaction of BPE with the Mg/Al (3/1) PMO was also carried out in 2:1 MeOH:DMC under the standard conditions. The result was analogous to the reaction in MeOH with the exception that the yield of anisole was substantially greater and that of phenol much less.

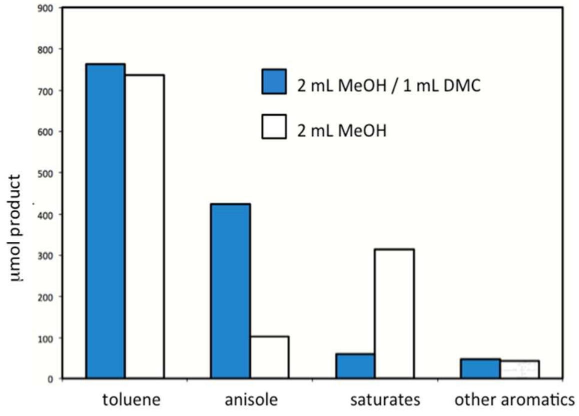

**Figure 7.** Changes in product distribution upon using dimethyl carbonate as a cosolvent vs using MeOH only. Products after 6 h reaction.

## Summary

The model systems quantitatively elucidated here clearly demonstrate four key substrate reactions catalysed by Cu20PMO under conditions where clean lignin and lignocellulose disassembly has been demonstrated.[21-23] Two of these are generally desirable, namely hydrogenolysis of aryl ether bonds and hydrodeoxygenation. The other two, aromatic hydrogenation and methylations of aromatic rings and of aliphatic carbons in positions adjacent to alcohol or ketone functionalities, lead to a proliferation of products, hence lower selectivity. Phenolic compounds, especially phenol, are susceptible to aromatic ring hydrogenation and methylation, thus are precursors to cyclohexanols that undergo subsequent methylation. In contrast, simpler aromatics such as benzene and toluene are relatively unreactive under analogous conditions as is anisole, which primarily undergoes slow HDO to benzene.

In this context, we have demonstrated that intercepting phenolic intermediates by alkylating the aromatic -OH dramatically reduces product proliferation and aromaticity loss. While this was accomplished using DMC as a cosolvent, these observations clearly point toward strategies that will enhance selectivity by addressing phenolic reactivity. Given the complexity of lignin as a substrate, any such strategy will inevitably give multiple products; however, narrowing the distribution will improve the eventual success of biological or chemical funnelling, hence the valorization of lignin.[1-4,45]

The essential role of copper in the methanol reforming that is the source of the reducing equivalents in the present system has been discussed previously.[21-23] However, the role of the supporting PMO is less well understood. Lewis acids have been shown to activate the aryl ether linkages to hydrogenolysis;[46-47] however, it is not clear how these would impact the other favourable and less favourable pathways of this catalytic system. For example, previous studies have demonstrated that mixed Mg/Al oxides catalyze phenol methylation.[38] Alternatively, methylation of the phenol oxygen, perhaps via catalysis by the acidic and basic sites at the support surface, would strongly affect overall reaction selectivity. Ongoing studies in our respective laboratories are addressing how the Cu-doped PMOs transform under the reaction conditions as well as how modifications of the support define reactivity and selectivity.

## Acknowledgements

We thank the Center for the Sustainable Use of Renewable Feedstocks (CenSURF), a NSF Center for Chemical Innovation (NSF CHE-1240194) for support of this research.

We also thank Megan Chui for catalyst preparation.

**Corresponding Authors**

* k.barta@rug.nl; ford@chem.ucsb.edu

## Notes and references

§ Various pathways can be envisioned for HDO depending on the substrate, including direct hydrogenolysis of C-OR bonds and dehydration followed by hydrogenation of the resulting unsaturated species.

1 A. J. Ragauskas, G. T. Beckham, M. J. Biddy, R. Chandra, F. Chen, M. F. Davis, B. H. Davison, R. A. Dixon, P. Gilna, M. Keller, P. Langan, A. K. Naskar, J. N. Saddler, T.J. Tschaplinski, G. A. Tuskan, C.E. Wyman, Lignin Valorization: Improving Lignin Processing in the Biorefinery. *Science*, 2014, **344**, 709.

2 C.O. Tuck, E. Perez, I. T. Horvath, R. A. Sheldon, M. Poliakoff, Valorization of Biomass: Deriving More Value from Waste. *Science*, 2012, **337**, 695-699.

3 J. Zakzeski, P. C. A. Bruijnincx, A. L. Jongerius, B. M. Weckhuysen, The Catalytic Valorization of Lignin for the Production of Renewable Chemicals. *Chem. Rev.*, 2010, **110**, 3552-3599.

4 P. Azadi, O. R. Inderwildi, R. Farnood, D. A. King, Liquid fuels, hydrogen and chemicals from lignin: A critical review. Renew. *Sust. Energ. Rev.* 2013, **21**, 506-523.

5 Y-C. Lin, G. W. Huber, The critical role of heterogeneous catalysis in lignocellulosic biomass conversion, *Energy Environ. Sci.*, 2009, **2** , 68-80.

6 T. Werpy, G. Petersen, *Top Value Added Chemicals from Biomass, Volume II – Results of Screening for Potential Candidates from Biorefinery Lignin.* Pacific Northwest National Laboratory and the National Renewable Energy Laboratory, 2007.

7 P. Sannigrahi, A. J. Ragauskas, G. A. Tuskan, Poplar as a Feedstock for Biofuels: A Review of Compositional Characteristics. Biofuels, *Bioprod. Bioref.* 2010, **4**, 209-226.

8 W. Boerjan, J. Ralph, M. Baucher, Lignin Biosynthesis. *Annu. Rev. Plant Biol.*, 2003, **54**, 519-546.

9 J. J. Stewart, T. Akiyama, C. Chapple, J. Ralph, S. D. Mansfield, The Effects on Lignin Structure of Overexpression of Ferulate 5-Hydroxylase in Hybrid Poplar. *Plant Physiol.*, 2009, **150**, 622-635.

10 R. Lal, Soils and Sustainable Agriculture: a Review. *Agronomy for Sustainable Development*, 2008, **28**, 15-22.

11 Global Aromatic Chemicals (Benzene, Toluene & Xylene) Market 2014. http://www.researchandmarkets.com/research/ 6xr4ck/global_aromatic (accessed Jan 29, 2015).

12 A. G. Pemba, M. Rostagno, A. L. Tanner, S. A. Miller, Cyclic and Spirocyclic Polyacetal Ethers from Lignin-Based Aromatics. *Polym. Chem.*, 2014, **5**, 3124-3221.

13 B. Sedai, C. Díaz-Urrutia, R. T. Baker, R. Wu, L. A. Silks, S. K. Hanson, Aerobic Oxidation of **β**□1 Lignin Model Compounds with Copper and Oxovanadium Catalysts, *ACS Catal.* 2013, B, 3111–3122.

14 S. Van den Bosch, W. Shutyser, R. Vanholme, T. Driessen, S.-F. Koelewijn, T. Renders, B. De Meester, W. J. J. Huijgen, W. Dehaen, C. M. Courtin, B. Lagrain, W. Boerjan, B. F. Sels, Reductive Lignocellulose Fractionation into Soluble Lignin-Derived Phenolic Monomers and Dimers and Processable Carbohydrate Pulps. *Energy Environ. Sci.*, 2015, DOI: 10.1039/C5EE00204D.

**15** R. Ma, W. Hao, X. Ma, Y. Tian, Y D. Li, Catalytic Ethanolysis of Kraft Lignin into High-Value Small-Molecular Chemicals over a Nanostructured alpha-Molybdenum Carbide Catalyst *Angew. Chem. Int. Ed.* 2014. **53,** 7310-7315

16 J. Zhang, Y. Chen, M. A. Brook, Reductive Degradation of Lignin and Model Compounds by Hydrosilanes. *ACS Sustainable Chem. & Eng. 2014*, **2**, 1983-1991

17 A. K Deepa, P. L. Dhepe, Lignin Depolymerization into Aromatic Monomers over Solid Acid Catalysts. ACS Catal. *2015*, **5**, 365-379

18 A. Rahimi, A. Ulbrich, J, J. Coon, S. S. Stahl, Formic-acid-induced depolymerization of oxidized lignin to aromatics *Nature*, *2014*, **515**, 249-252

19 Y. Jiang, Z. Li, X. Tang, Y. Sun, X. Zeng, S. Liu, L. Lin, Depolymerization of Cellulolytic Enzyme Lignin for the Production of Monomeric Phenols over Raney Ni and Acidic Zeolite Catalysts. *Energy & Fuels, 2015*, **29**, 1662-166

20 M. R. Sturgeon, M. H. O'Brien, P. N. Ciesielski, R. Katahira, J. S. Kruger, S. C. Chmely, J. Hamlin, K. Lawrence, G. B. Hunsinger, T. D. Foust, R. M. Baldwin, M. J. Biddy, G. T. Beckham, Lignin depolymerisation by nickel supported layered-double hydroxide catalysts. *Green Chem. 2014*, **16**, 824-835

21 K. Barta, T. D. Matson, M. L. Fettig, S. L. Scott, A. V. Iretskii, P. C. Ford, Catalytic Disassembly of an Organosolv Lignin via Hydrogen Transfer from Supercritical Methanol. *Green Chem.*, 2010, **12**, 1640.

22 T. D. Matson, K. Barta, A. V. Iretskii, P. C. Ford, One-Pot Catalytic Conversion of Cellulose and of Woody Biomass Solids to Liquid Fuels. *J. Am. Chem. Soc.*, 2011, **133**, 14090-14097.

23 K. Barta, P. C. Ford, Catalytic Conversion of Non-food Woody Biomass Solids to Organic Liquids. *Acc. Chem. Res.*, 2014, **47**, 1503−1512.

24 G. S. Macala, T. D. Matson, C. L. Johnson, R. S. Lewis, A. V. Iretskii, P. C. Ford, Hydrogen Transfer from Supercritical Methanol Over a Solid Base Catalyst: a Model for Lignin Depolymerization. *Chem. Sus. Chem.*, 2009, **2**, 215–217.

25 S. Lee, *Methanol Synthesis Technology*, CRC Press: Boca Raton, Florida, 1990.

26 A. A. Gokhale, J. A. Dumesic, M. Mavrikakis, On the Mechanism of Low-Temperature Water Gas Shift Reaction on Copper. *J. Am. Chem. Soc.*, 2008, **130**, 1402–1414.

27 K. Barta, G. R. Warner, E. S. Beach, P. T. Anastas, Depolymerization of Organosolv Lignin to Aromatic Compounds Over Cu-Doped Porous Metal Oxides. *Green Chem.*, 2014, **16**, 191-196.

28 T. S. Hansen, K. Barta, P. T. Anastas, P. C. Ford, A. Riisager, One-pot reduction of 5-hydroxymethylfurfural via hydrogen transfer from supercritical methanol. *Green Chem.*, 2012, **14**, 2457-2461.

29 A. J. Kumalaputri, G. Bottari, P. M. Erne, H. J. Heeres, K. Barta, Tunable and Selective Conversion of 5-HMF to 2, 5-Furandimethanol and 2, 5-Dimethylfuran over Copper-Doped Porous Metal Oxides. *Chem. Sus. Chem.*, 2014, **7**, 2266-2275.

30 X. Huang, T. I. Koranyi, M. D. Boot, E. J. M. Hensen, Catalytic Depolymerization of Lignin in Supercritical Ethanol. *Chem. Sus. Chem.*, 2014, **7**, 2276–2288.

31 M. J. Girgis, B. C. Gates, Reactivities, Reaction Networks, and Kinetics in High-Pressure Catalytic Hydroprocessing. *Ind. Eng. Chem. Res.*, 1991, **30**, 2021-2058.

32 R. C. Runnebaum, T. Nimmanwudipong, D. E. Block, B. C. Gates, Catalytic conversion of compounds representative of lignin-derived bio-oils: a reaction network for guaiacol, anisole, 4-methylanisole, and cyclohexanone conversion catalysed by Pt/gamma-Al2O3. *Catal. Sci. Technol.*, 2012, **2**, 113-118.

33 Q. Bu, H. Lei, A. H. Zacher, L. S. Ren, J. Liang, Y. Wei, Y. Liu, J. Tang, Q. Zhang, R. Ruan, A review of catalytic hydrodeoxygenation of lignin-derived phenols from biomass pyrolysis. *Bioresour. Technol.*, 2012, **124**, 470–477.

34 X. Wang, R. Rinaldi, Route for Lignin and Bio-Oil Conversion: Dehydroxylation of Phenols into Arenes by Catalytic Tandem Reactions. *Angew. Chem. Int. Ed.*, 2013, **52**, 11499 –11503.

35 X. Wang, R. Rinaldi, Exploiting H-transfer reactions with RANEY (R) Ni for upgrade of phenolic and aromatic biorefinery feeds under unusual, low-severity conditions, *Energy Environ. Sci.*, 2012, **5**, 8244-8260.

36 J. T. Scanlon, D. E. Willis, Calculation of Flame Ionization Detector Relative Response Factors Using the Effective Carbon Number Concept. *J. Chromatogr. Sci.*, 1985, **23**, 333-340.

37 P. Kuzmic, Program DYNAFIT for the Analysis of Enzyme Kinetic Data: Application to HIV Proteinase. *Anal. Biochem.*, 1996, **237**, 260-273.

38 V. Crocella, G. Cerrato, G. Magnacca, C. Morterra, F. Cavani, L. Maselli, S. Passeri, Gas-phase Phenol Methylation of Mg/Me/O (Me=Al, Cr, Fe) Catalysts: Mechanistic Implications Due to Different Acid-Base and Dehydrogenating Properties. *Dalton Trans.*, 2010, **39**, 8527-8537.

39 K. L. Deutsch, B. H. Shanks, Hydrodeoxygenation of Lignin Model Compounds Over a Copper Chromite Catalyst. *App. Cat.*, 2012, **447**, 144– 150.

40 W. Song, Y. Liu, E. Baráth, C. Zhao, J. A. Lercher, Synergistic effects of Ni and acid sites for hydrogenation and C-O bond cleavage of substituted phenols. *Green Chem.*, 2015, **17**, 1204-1218.

41 A. W. Pelzer, M. R. Sturgeon, A. J. Yanez, G. Chupka, M. H. O'Brien, R. Katahira, R. D. Cortright, L. Woods, G. T. Beckham, L. J. Broadbelt, Acidolysis of the α-O-4 Aryl-Ether Bonds in Lignin Model Compounds: A Modeling and Experimental Study. *ACS Sustain. Chem. Eng.*,2015, **3**, 1339-1347.

42 R. Luque, J. M. Campelo, T. D. Conesa, D. Luna, J. M. Marinas, A. A. Romero, Catechol O-Methylation with Dimethyl Carbonate Over Different Acid-Base Catalysts. *New. J. Chem.*, 2006, **30**, 1228-1234.

43 M. B. Talawar, T. M. Jyothi, P. D. Sawant, T. Raja, B. S. Rao, Calcined Mg-Al Hydrotalcite as an Efficient Catalyst for the Synthesis of Guaiacol. *Green Chem.*, 2000, **2**, 266-268.

44 J. N. G. Stanley, M. Selva, A. F. Masters, T. Maschmeyer, A. Perosa, Reactions of p-coumaryl alcohol model compounds with dimethyl carbonate. Towards the upgrading of lignin build-ing blocks. *Green Chem.*, 2013, **15**, 3195-3204.

45 J. G. Linger, D. R. Vardon, M. T. Guarnieri, E. M. Karp, G. B. Hunsinger, M. A. Franden, C. W. Johnson, G. Chupka, T. J. Strathmann, P. T. Pienkos, G. T. Beckham, Lignin valorization through integrated biological funneling and chemical catalysis, *Proc. Nat. Acad. Sci.*, 2014, **111**, 12013-12018.

46 A. C. Atesin, N. A. Ray, P.C. Stair, T. J. Marks, Ether C-O Bond Hydrogenolyiss Using a Tandem Lanthanide Triflate/Supported Palladium Nanoparticle Catalyst System. *J. Am. Chem. Soc.*, 2012, **134**, 14682-14685.

47 T. H. Parsell, B. C. Owen, T. M. Jarell, C. L. Marcum, L. J. Haupert, L. M. Amundson, K. I. Kenttamaa, F. Ribeiro, J. T. Miller, M. M. Abu-Omar, Cleavage and Hydrodeoxygenation (HDO) of C-O Bonds Relevant to Lignin Conversion Using Pd/Zn Synergistic Catalysis. *Chem. Sci.*, 2013, **4**, 806-813.

## Graphical Abstract

Global kinetics analysis for reduction of lignin models catalyzed by Cu-PMOs identifies targets for rational design to enhance selectivity.